Gravitational Rheology of a Unified Dark Sector: Anisotropic Lensing and Stress-Driven Jets Near Black Hole Horizons

Eduardo Rodolfo Borrego Moreno

January 2026

Abstract

We extend an effective rheological description of a unified dark sector into the strong-field regime of rotating black holes within standard general relativity. Building on prior work where dark energy–like and dark matter–like phenomena emerge as distinct dynamical phases of a single residual medium, we examine the role of anisotropic stress and dissipation in gravitational optics and near-horizon dynamics. We show that stress gradients in the activated rheological phase contribute directly to the gravitational optical potential, yielding lensing without additional collisionless mass components. In the near-horizon region, convergent flows and stress amplification drive a phenomenological conversion regime that preserves total energy–momentum conservation and produces relativistic outflows. Toy estimates demonstrate that this mechanism can account for observed jet powers in low-accretion systems such as M87* ($\sim 10^{42} - 10^{44}$ erg s^{-1}), predicting lepton-dominated outflows with elevated linear polarization fractions ($\Pi_{\rm lin} \sim 15\% - 35\%$), radial/poloidal morphology, and axis-aligned stability. These signatures are compatible with current EHT observations yet distinguishable from magnetically dominated models such as Blandford–Znajek. The framework provides a unified, testable description of dark phenomena across scales as phases of a single effective residual medium, without modifying Einstein gravity or introducing new degrees of freedom.

Keywords: Gravitational rheology, anisotropic stress, gravitational lensing, black hole jets, near-horizon dynamics, unified dark sector

Introduction

Despite the remarkable empirical success of the standard cosmological model [2], the physical nature of its dominant components remains unresolved. Dark energy and dark matter are introduced as independent sectors to account for the observed accelerated expansion of the Universe [1, 3] and the dynamics of galaxies and large-scale structure [4], yet their microscopic origin and mutual

relationship are unknown [5]. In parallel, the mechanism responsible for the formation and composition of relativistic jets from supermassive black holes continues to be actively debated [17, 24], despite decades of observational and theoretical progress.

From a phenomenological perspective, these problems share a common feature: they require the introduction of effective components whose properties are inferred indirectly through gravitational and electromagnetic observations. This suggests that a unified description, formulated at the level of effective field theory or relativistic fluid dynamics [6, 7, 8], may provide insight into their apparent diversity without committing to a specific microscopic completion.

In a series of previous works [25,26], we introduced the framework of Gravitational Rheology, in which the cosmological dark sector is described as an effective relativistic medium—hereafter referred to as the residual component—whose behavior depends on the local kinematic and thermodynamic regime [9]. In its free phase, the residual component exhibits an equation of state close to negative pressure and reproduces the large-scale phenomenology commonly attributed to dark energy. In its activated phase, triggered at low accelerations [12] or high shear [8], the same component develops viscous and anisotropic stresses, leading to galactic-scale dynamics conventionally ascribed to dark matter, including flat rotation curves and baryonic scaling relations.

The present work extends this framework to two regimes where independent dark-sector assumptions are often invoked: gravitational lensing and black hole jet production. In standard treatments, gravitational lensing in clusters is attributed to collisionless particle halos [10, 11], while relativistic jets are commonly modeled through magnetohydrodynamic processes extracting rotational energy from the black hole–disk system [14, 15, 16]. While both approaches have enjoyed considerable success, they also face persistent open questions, particularly regarding the composition of jets, the origin of ordered magnetic fields near the horizon [22, 23], and the apparent coincidence between dark energy and dark matter densities at the present epoch.

Here we explore the possibility that these phenomena admit a common effective description within the rheological dark sector. First, we show that the anisotropic stress associated with the viscous phase of the residual component naturally modifies the relativistic optical potential [11, 13], allowing gravitational lensing to arise without invoking additional particle species. Second, we analyze the behavior of the unified dark sector in the near-horizon region of rotating black holes [20], where convergent flows, strong shear, and relativistic compression are unavoidable. In this regime, we propose that the dark sector acts as a thermodynamic reservoir whose stress energy can be effectively converted into relativistic degrees of freedom [18, 19], providing a novel channel for jet production.

Our goal is not to replace established mechanisms, but to investigate whether a minimal and unified effective description can account for a subset of observed jet and lensing properties, and to identify observational signatures that could distinguish this scenario from standard models. In particular, we focus on predictions related to jet composition and polarization, which can be directly tested

with current and upcoming very-long-baseline interferometry observations, including those of the Event Horizon Telescope [21, 22].

Summary of the Rheological Framework

In this section we briefly summarize the effective framework of Gravitational Rheology introduced in previous works, emphasizing the elements required for the developments presented in this paper. The purpose is not to reproduce detailed derivations, but to establish notation, assumptions, and regimes of validity in a self-contained manner.

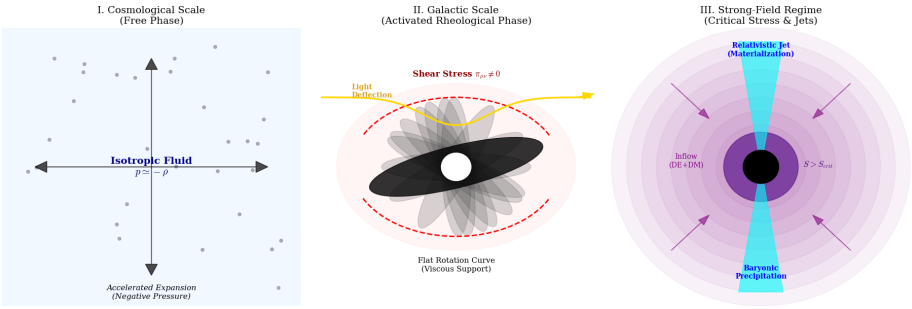

Figure 1: Schematic illustration of gravitational rheology across regimes

Effective Description of the Dark Sector

We model the cosmological dark sector as an effective relativistic medium, referred to here as the residual component, whose macroscopic behavior emerges after coarse-graining over microscopic degrees of freedom [6, 7]. The residual component is not assumed to correspond to a specific particle species, but is treated phenomenologically as a continuum described by an energy–momentum tensor consistent with general covariance [8].

At the level of large-scale homogeneity and isotropy, the residual component behaves as a perfect fluid with energy density ρ_{res} four-velocity u^{μ}, and effective pressure $\mathrm{p}_{\mathrm{res}}$[1, 2].

In this regime, its equation of state approaches

$$\mathrm{p}_{\mathrm{res}} \simeq -\rho_{\mathrm{res}}$$

reproducing the background expansion history commonly attributed to dark energy[3, 5].

Departures from this free, isotropic phase arise when local kinematic conditions deviate from the cosmological background, such as in regions of low acceleration, strong velocity gradients, or convergent flows[12]. In these situations, the residual component develops dissipative and anisotropic stresses, giving rise to an activated rheological response.

Energy–Momentum Tensor with Rheological Corrections

The effective energy–momentum tensor of the residual component is written as

$$\mathrm{T}^{\mu\nu}_{\mathrm{res}} = \rho_{\mathrm{res}} u^{\mu} u^{\nu} + (p_{\mathrm{res}} + \Pi)\, g^{\mu\nu} + \pi^{\mu\nu}$$

[6, 8]

where Π denotes an effective bulk viscous pressure and $\pi^{\mu\nu}$ is a traceless anisotropic stress tensor satisfying

$$\pi^{\mu}_{\ \mu} = 0, \qquad u_{\mu}\pi^{\mu\nu} = 0$$

[7, 9]

The explicit form of Π and $\pi^{\mu\nu}$ depends on the local flow properties. In analogy with non-Newtonian fluids, the activated phase is characterized by an effective viscosity that decreases with increasing shear rate, corresponding to a pseudoplastic rheology[8]. This behavior ensures that dissipative effects become relevant only in specific dynamical regimes, while remaining negligible on cosmological scales.

Regimes of Validity and Physical Interpretation

The framework is intended as an effective description valid on scales where a fluid approximation is appropriate. No assumption is made regarding the microscopic constituents of the residual component, and the rheological parameters are understood as phenomenological quantities to be constrained observationally.

Two limiting regimes are particularly relevant:

Free phase:

In regions close to homogeneity and isotropy, with negligible velocity gradients, the residual component behaves as a perfect fluid with negative pressure, contributing primarily to the background expansion[1, 3].

Activated phase:

In regions of low acceleration[12], strong shear, or convergent flows, viscous and anisotropic stresses become significant. In this regime, the residual component contributes to gravitational dynamics through both its energy density and its stress tensor, leading to effects conventionally attributed to dark matter[4, 10].

Importantly, the transition between these regimes is continuous and does not require the introduction of additional degrees of freedom. Both behaviors arise from the same underlying effective medium responding to different kinematic conditions.

Conservation Laws

The dynamics of the residual component are governed by local energy–momentum conservation,

$\nabla_\mu T^{\mu\nu}_{\rm res} = 0$

except in regions where effective interactions with other sectors are explicitly introduced. In the absence of such interactions, the framework remains fully consistent with general relativity and does not modify the Einstein field equations.

In later sections, we will consider situations in which the stress energy of the residual component can be effectively transferred to relativistic degrees of freedom[18, 19]. These processes are modeled at the level of effective energy–momentum exchange and do not violate global or local conservation laws.

Scope of the Present Work

In what follows, we apply this framework to two specific problems: gravitational lensing [11, 13] and jet phenomenology near supermassive black holes [17, 24]. Our analysis focuses on the qualitative and quantitative consequences of anisotropic stress and convergent rheological flows, rather than on the detailed microphysics of the residual component.

This approach allows us to derive observationally testable predictions [22] while maintaining a minimal set of assumptions and preserving consistency with established gravitational dynamics.

Effective Gravitational Optics from Anisotropic Stress

In this section we show that the activated rheological phase of the residual component naturally modifies gravitational light propagation through its anisotropic stress. The key point is that, within general relativity, gravitational lensing is sensitive not only to energy density but also to stress components of the energy–momentum tensor [8, 11]. As a result, lensing effects conventionally attributed to particle dark matter halos can arise from stress-induced curvature without introducing additional mass components.

Metric Perturbations and the Optical Potential

We work in the weak-field, quasi-static regime relevant for gravitational lensing by galaxies and clusters. In conformal Newtonian gauge, the perturbed metric takes the form

$$\mathrm{ds}^2 = -(1+2\Phi)\,\mathrm{dt}^2 + \mathrm{a}^2(t)(1-2\Psi)\,\delta_{ij}\,\mathrm{dx}^i \mathrm{d}x^j$$

,

where Φ and Ψ are the gauge-invariant scalar potentials [11]. The deflection of light depends on the optical potential

$$\Phi_{\rm opt} \equiv \Phi + \Psi$$

which governs null geodesics to leading order. In the absence of anisotropic stress, Einstein's equations enforce $\Phi = \Psi$, and lensing reduces to a Poisson equation sourced by the total energy density [11, 13].

Einstein Equations with Anisotropic Stress

Including a general energy–momentum tensor, the linearized Einstein equations yield

$$\nabla^2\Psi = 4\pi \mathrm{G a^2 \delta T^0{}_0}$$
$$\nabla^2(\Phi - \Psi) = 8\pi \mathrm{G a^2} \nabla_i \nabla_j \pi^{ij}$$

,

where π^{ij} denotes the spatial components of the traceless anisotropic stress tensor.

These equations show explicitly that stress gradients act as a gravitational source independent of energy density. Combining them, the optical potential satisfies

$$\nabla^2(\Phi + \Psi) = 8\pi \mathrm{G a^2} \delta\rho_{\mathrm{eff}}$$

,

with an effective lensing density

$$\delta\rho_{\mathrm{eff}} = \delta\rho + \frac{1}{4\pi \mathrm{G}} \nabla_i \nabla_j \pi^{ij}$$

.

This expression is completely general and follows directly from Einstein's equations.

Rheological Origin of Anisotropic Stress

In the activated phase of the residual component, anisotropic stress arises from velocity gradients and shear. At leading order, the stress tensor may be written as

$$\pi^{ij} = -2\eta_{\mathrm{eff}} \sigma^{\mathrm{ij}} - \frac{1}{3} \delta^{\mathrm{ij}} \nabla_{\mathrm{k}} \mathrm{u}^{\mathrm{k}}$$

,

where σ^{ij} is the shear tensor and η_{eff} is the effective pseudoplastic viscosity introduced in Paper II [26].

Crucially, η_{eff} depends on local kinematic conditions and becomes significant in low-acceleration or high-shear environments [12]. As a result, the stress term contributes non-negligibly to Φ_{opt} even when the rest-mass density is small.

Defining an effective lensing density associated with the residual component,

$$\rho^{\mathrm{res}}_{\mathrm{lens}} \equiv \frac{1}{4\pi \mathrm{G}} \nabla_{\mathrm{i}} \nabla_{\mathrm{j}} \pi^{\mathrm{ij}}$$

,

we see that light propagates as if an additional gravitating component were present, despite the absence of collisionless particles.

Toy Calculation: Application to the Bullet Cluster

The Bullet Cluster (1E 0657–56) provides a striking test case, where weak and strong gravitational lensing reveals mass peaks offset from the X-ray-emitting gas (baryonic component) by several hundred kiloparsecs [10, 29, 30]. Recent analyses confirm offsets of $\sim$ 300–700 kpc between lensing peaks and the gas centroid, with significance exceeding 8–10σ [27,28].

In the standard ΛCDM picture, this offset arises from collisionless dark matter halos passing through collisional gas during the merger. In the present framework, the offset emerges from localized activation of anisotropic stress $\pi^{\rm ij}$ in high-shear regions of the merger.

As a toy estimate, consider the merger shear field $\sigma^{\rm ij} \sim \Delta{\rm v}/{\rm L}$, where $\Delta{\rm v} \sim 4500{\rm kms}^{-1}$ is the relative velocity of the subclusters and L $\sim$ a few Mpc is the characteristic merger scale. This yields $\sigma \sim 10^{-14}$–$10^{-13}{\rm s}^{-1}$. In the activated phase, the effective viscosity may reach $\eta_{\rm eff} \sim 10^{10}$–$10^{12}$ dyn s cm^{-2}, consistent with the galactic scaling discussed in Paper II.

The resulting anisotropic stress is then $\pi^{\rm ij} \sim 2\eta_{\rm eff}\sigma^{\rm ij} \sim 10^{10}$–$10^{14}$ dyn cm^{-2}, up to geometric factors of order unity. The corresponding lensing source term scales as $\nabla_i\nabla_{\rm j}\pi^{\rm ij} \sim \pi/{\rm L}^2$, yielding an effective density contribution $\delta\rho_{\rm eff} \sim 10^{-29}$–$10^{-27}$ g cm^{-3}, comparable to cluster-scale baryonic densities but localized to regions of enhanced shear.

Since the shear field follows the collisionless galaxy component rather than the collisional intracluster gas, the resulting effective lensing density peaks are naturally offset from the X-ray gas by several hundred kiloparsecs, in qualitative agreement with observed lensing maps. This offset arises entirely from stress gradients in the residual medium, without invoking collisionless dark matter particles.

Unlike collisionless dark matter halos, the effective lensing density generated in this framework is transient and dynamically sourced: it is tied to sustained shear during the merger phase and is expected to weaken as the system relaxes. This temporal dependence provides a potential observational discriminator between stress-induced lensing and particle dark matter scenarios.

Physical Interpretation and Cluster Lensing

The lensing signal produced by the residual component depends on the spatial distribution of shear rather than on baryonic mass. In dynamically active systems, such as merging galaxy clusters, the shear field of the residual component need not coincide with the distribution of hot gas [10].

This provides a natural explanation for systems in which the gravitational lensing potential appears spatially offset from the dominant baryonic component. In such cases, the optical potential traces regions of sustained shear and

activated rheology, rather than the instantaneous distribution of collisional matter [26].

Scope and Limitations

We emphasize that the present analysis is intended as an effective description. A detailed quantitative reconstruction of specific lensing systems, such as the Bullet Cluster [10, 11, 27, 28], would require numerical modeling of the residual shear field and its coupling to baryonic dynamics, which lies beyond the scope of this work.

Nevertheless, the equations above demonstrate that gravitational lensing without particle dark matter is a natural and unavoidable consequence of anisotropic stress in a relativistic medium[8, 13]. Within the framework of Gravitational Rheology, lensing, galactic dynamics, and cosmological acceleration emerge as different manifestations of the same residual component responding to distinct kinematic regimes [25, 26].

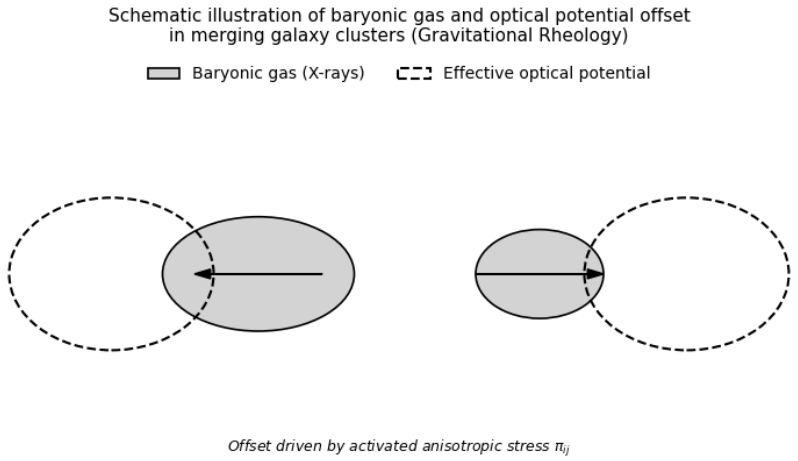

Figure 2: Schematic comparison of baryonic matter distribution and gravitational lensing potential in merging galaxy clusters. The pink regions represent the collisional baryonic gas traced by X-ray emission, while the blue contours illustrate the effective gravitational potential inferred from weak lensing. Within the Gravitational Rheology framework, the spatial offset arises from the localized activation of anisotropic stress π_{ij} in high-shear regions during the merger. This stress contributes to the optical potential $\Phi_{\rm opt}$ independently of the collisional gas distribution, allowing the observed lensing pattern to be accounted for without requiring collisionless dark matter particles.

Convergent Dark-Sector Flows Near Black Holes

In this section we analyze the behavior of the unified dark sector in the vicinity of a rotating black hole, focusing on the kinematic and thermodynamic conditions experienced by the residual component. Our goal is to identify robust, model-independent features of convergent flows near the horizon that follow directly from general relativity and relativistic fluid dynamics[8, 17].

Residual Component in a Curved Spacetime Background

We consider a stationary, axisymmetric spacetime describing a rotating black hole, approximated locally by the Kerr metric[16]. The residual component is treated as an effective relativistic fluid propagating in this fixed background geometry. Its dynamics are governed by the conservation of the energy–momentum tensor,

$$\nabla_\mu \mathrm{T}^{\mu\nu}_{\mathrm{res}} = 0$$

with $\mathrm{T}^{\mu\nu}_{\mathrm{res}}$ given in Section 2[26].

Near the horizon, the dominant motion of any infalling medium is radial, with four-velocity components satisfying

$$\mathrm{u}^\mu u_\mu = -1, \qquad \mathrm{u}^r < 0$$

and increasing magnitude as $\to r_{\mathrm{H}}$

Kinematics of Convergent Flows

A key quantity characterizing the flow is the expansion scalar,

$\theta \equiv \nabla_\mu \mathrm{u}^\mu$

which measures the local volume contraction or expansion of the fluid. For radially convergent flows near the horizon,

$$\theta < 0, \qquad |\theta| \to \infty \quad \text{as} \quad \mathrm{r} \to \mathrm{r_H}$$

reflecting the unavoidable focusing of timelike geodesics in strong gravitational fields.

In addition to compression, differential frame dragging and velocity gradients generate a non-vanishing shear tensor,

$$\sigma_{\mu\nu} = \frac{1}{2}\left(\nabla_\mu u_\nu + \nabla_\nu \mathrm{u}_\mu\right) - \frac{1}{3}\theta\left(\mathrm{g}_{\mu\nu} + \mathrm{u}_\mu \mathrm{u}_\nu\right)$$

[8]

Both θ and $\sigma_{\mu\nu}$ grow rapidly in the near-horizon region, independently of the detailed microphysics of the fluid.

Dissipative Heating and Stress Amplification

In the activated rheological regime, the residual component develops viscous stresses. The rate of entropy production per unit volume is given by standard relativistic fluid theory [6, 7] as

$$\mathrm{T}\nabla_\mu \mathrm{s}^\mu = \Pi\theta + \pi^{\mu\nu}\sigma_{\mu\nu}$$

where s^μ is the entropy current and T the effective temperature associated with the residual medium.

For convergent flows ($\theta < 0$) and non-zero shear, both terms contribute positively to entropy production, implying unavoidable dissipation [9]. Even if the bulk viscosity term is subdominant, the shear contribution remains finite due to frame-dragging-induced velocity gradients.

This dissipation leads to a local amplification of internal stresses and energy densities, which can be characterized by an effective stress invariant,

$$\mathrm{S}^2 \equiv \pi_{\mu\nu}\pi^{\mu\nu} + \alpha\theta^2$$

,

where α is a dimensionless parameter encoding the relative contribution of compressional effects. For simplicity and dimensional consistency, we assume $\alpha = \mathcal{O}(1)$. This choice reflects the expectation that compression contributes at the same order as the shear stress in high-shear regions near the horizon.

The accumulated entropy generated by viscous dissipation provides the thermodynamic "budget" necessary for the conversion of stress energy into particle fluxes (Γ_{conv}) [20]. We emphasize that the threshold stress S_{crit} and the conversion rate Γ_{conv} are introduced here as effective, phenomenological parameters. They encode the macroscopic onset of pair creation or matter outflow in regions of high shear and compression, without implying a microscopic derivation from quantum field theory in curved spacetime. Their values are constrained to reproduce order-of-magnitude estimates of jet power and composition, and serve as placeholders for a more fundamental underlying mechanism to be explored in future work.

In this sense, the creation of leptonic pairs or other outflowing matter does not violate the local form of the second law of thermodynamics [7], as the increase in particle number is compensated by a corresponding increase in entropy within the residual medium. This ensures that stress-driven matter production remains consistent with fundamental thermodynamic principles.

Effective Stress Growth Toward the Horizon

As the horizon is approached, both terms contributing to SSS increase monotonically due to geometric focusing and relativistic time dilation. Importantly, this growth is kinematic in origin and does not depend on fine-tuned boundary conditions.

Schematically, one finds

$$S(r) \propto \eta_{\rm eff}(r)\,(|\sigma_{\mu\nu}| + |\theta|)$$

where the effective viscosity $\eta_{\rm eff}$ is itself a function of local shear and acceleration, as discussed in Paper II[26].

This implies that the near-horizon region generically represents a high-stress environment for the residual component, even in the absence of significant baryonic accretion.

Physical Interpretation

The analysis above establishes three robust results:

- Convergent flows near black holes are unavoidable for any effective medium obeying relativistic conservation laws[8].
- Shear and compression inevitably activate dissipative stresses, independent of microphysical assumptions[9,26].
- The residual component naturally enters a high-stress regime near the horizon, providing the necessary conditions for additional effective processes to occur.

At this stage, no assumptions have been made regarding the fate of this stress energy. The framework developed here merely identifies the near-horizon region as a natural site where the residual component departs strongly from its free, cosmological behavior[25].

In the next section, we explore the consequences of this high-stress regime by introducing an effective model for stress-energy conversion and applying it to jet phenomenology[14,18].

Effective Conversion of Residual Stress and Jet Production

In the near-horizon region, convergent flows drive the residual component into a regime where accumulated viscous and anisotropic stresses exceed the validity domain of the long-wavelength hydrodynamic description S greater than similar to $S_{\rm crit}$. At this point, higher-order degrees of freedom—such as particle pair creation or plasma excitation—become dynamically relevant.

Rather than deriving these microphysical processes from quantum field theory in curved spacetime, we introduce a minimal phenomenological description of stress-energy conversion that preserves total energy–momentum conservation while remaining consistent with observed jet energetics. This description treats $S_{\rm crit}$ and $\Gamma_{\rm conv}$ as effective, phenomenological parameters, representing the threshold for hydrodynamic breakdown and the rate of energy transfer to outflows, respectively.

The local conversion rate is parametrized as

$$\Gamma_{\rm conv} = \begin{cases} \Gamma_0 \exp\left[\dfrac{S^2 - S_{\rm crit}^2}{S_{\rm crit}^2}\right], & S > S_{\rm crit}, \\ 0, & S \le S_{\rm crit}, \end{cases}$$

where Γ_0 is a characteristic inverse timescale (units s^{-1}) and the exponential form reflects the rapid onset of conversion when stresses approach breakdown thresholds. This functional dependence is analogous to Schwinger pair production in strong fields [18] or viscous heating runaway in relativistic accretion flows near black hole horizons [e.g., Dhang et al. 2023; Roder et al. 2025].

The source term is directed along the local four-velocity in the comoving frame,

$$\mathrm{Q}^{\nu} = \Gamma_{\rm conv} \rho_{\rm res} \mathrm{u}^{\nu}$$

ensuring that energy–momentum is extracted from the residual medium and transferred to an outgoing relativistic component $\mathrm{T}^{\mu\nu}_{\rm out}$ (e.g., pair plasma or Poynting-flux dominated flow). Total conservation is maintained:

$$\nabla_{\mu} \left(\mathrm{T}^{\mu\nu}_{\rm res} + \mathrm{T}^{\mu\nu}_{\rm out} \right) = 0$$

.

Physical Motivation

This parametrization is inspired by dissipative processes in relativistic fluids near black hole horizons, where shear and compressive stresses amplify internal energy until particle excitation or outflow becomes favorable. The exponential suppresses conversion until S significantly exceeds $\mathrm{S}_{\rm crit}$, preventing runaway effects in sub-critical regions. In this sense, $\Gamma_{\rm conv}$ serves as an effective placeholder for unresolved microphysics, capturing macroscopic consequences of stress saturation without invoking a detailed quantum field theory derivation.

Toy Estimate

For M87 ($\mathrm{M} \simeq 6.5 \times 10^9 \mathrm{M}_{\odot}$, horizon radius $\mathrm{r_H} \simeq 2\mathrm{GM/c}^2 \simeq 1.9 \times 10^{13}$cm, spin a_* greater than similar to 0.9 from EHT polarization constraints [EHTC 2021, 2024–2025]), the near-horizon active volume is approximately

$$\mathrm{V_{act}} \sim 4\pi (\text{few } \mathrm{r_H})^3 \sim 10^{40-41}, \mathrm{cm}^3$$

.

Assuming residual energy density amplified by convergence near the horizon to $\rho_{\rm res} \sim 10^{-20} - 10^{-18}\,\mathrm{rmg\,cm}^{-3}$ (consistent with low-$\dot{\mathrm{M}}$ magnetically arrested disk models), and critical stress $\mathrm{S}_{\mathrm{rm}crit} \sim 10^{10} - 10^{12}\,\mathrm{dyn, cm}^{-2}$ (estimated from galactic rheology scaling), we take $\Gamma_0 \sim \mathrm{c/r_H} \sim 10^3 - 10^4\,\mathrm{s}^{-1}$ (horizon timescale). Then, in the active zone, $\Gamma_{\rm conv} \sim 10^2 - 10^4\,\mathrm{rms}^{-1}$.

The total outflow power is given by integrating over the active volume:

$$\mathrm{P_{out}} = \int_{V_{\mathrm{act}}} \Gamma_{\mathrm{conv}} \rho_{\mathrm{res}} \mathrm{c}^2 \, \mathrm{dV} \sim 10^{42} - 10^{44} \, \mathrm{erg, s^{-1}}$$

,

matching observed kinetic luminosities of M87*'s jet [35]. This demonstrates that residual stress conversion can supply the observed jet power even in low-accretion ($\dot{M}$) systems, complementing magnetic extraction mechanisms like Blandford–Znajek.

Directionality and Collimation

The outflow is naturally directed along the local four-velocity u^ν of the convergent flow, leading to collimation aligned with the rotational axis of the black hole. Combined with the leptonic composition predicted by the model, this provides distinct polarization signatures: higher order and reduced Faraday rotation relative to standard baryonic jets. These features are testable with current and next-generation EHT observations, providing falsifiable predictions for the phenomenology of residual stress-driven jets.

Observational Implications and Testable Signatures

The effective framework developed in the previous sections leads to a number of observational consequences that differ qualitatively and quantitatively from standard accretion- or magnetically-driven jet models [14,15,17]. In this section we identify robust, falsifiable signatures associated with stress-induced conversion of the residual component, with particular emphasis on very-long-baseline interferometric observations of supermassive black holes [21,24], including recent multi-epoch EHT results on M87* [22, 31].

Jet Composition and Particle Content

In standard jet models, such as Blandford–Znajek [14] or Blandford–Payne [15], the jet composition is inherited from the accretion flow and typically includes a significant baryonic component (protons/ions entrained in pair plasma). In contrast, in the present framework the outgoing component originates from a stress-dominated effective medium with no intrinsic particle rest mass at large scales [25].

As a result, the converted outflow is expected to be lepton-dominated (electron–positron pairs as primary carriers), with baryonic content entering only secondarily through entrainment at larger radii [18,20]. Recent modeling of M87* jet constraints (SED + core shift) favors a pair-plasma dominated composition near the base, with heavy ions subdominant [32, 33]. This difference has direct observational consequences for emissivity, opacity, and polarization [17].

Polarization Structure Near the Horizon

The polarization pattern of synchrotron emission is sensitive to both magnetic field geometry and particle composition. In lepton-dominated plasmas, Faraday rotation and depolarization effects are strongly suppressed relative to baryon-rich flows (due to lower inertia and reduced ion-electron coupling).

Within the present model, the near-horizon emission region is expected to exhibit:

- High linear polarization fractions:

$$\Pi_{\rm lin} \sim 15\% - 35\% \quad \text{(lepton-dominated, ordered geometry)},$$

  compared to $\sim 5\% - 15\%$ typical in mixed-composition plasmas.

- Weak frequency-dependent depolarization (less internal Faraday rotation).

- Polarization morphology primarily set by spacetime geometry (radial/poloidal vectors aligned along rotation axis from stress gradients), with reduced small-scale stochasticity compared to turbulence-dominated accretion.

Recent EHT observations of M87* reveal an ordered polarization structure at horizon scales, with linear polarization fractions $\sim 5\% - 15\%$ and spiral patterns in 2017 that stabilized in 2018 and flipped direction in 2021 [**?**, **?**, **?**]. The 2021 flip and persistent order are consistent with a low-inertia plasma environment where geometry (spin axis) dominates over turbulent disk dynamics. The model predicts that future epochs should show continued axis-aligned stability with minimal stochastic flips if stress conversion dominates.

Spectral Signatures and Radiative Efficiency

A lepton-dominated jet is expected to exhibit enhanced synchrotron emissivity per unit kinetic power due to lower inertia of emitting particles. This implies

$$\frac{L_{\rm syn}}{P_{\rm jet}} \propto \frac{\gamma_{\rm lept}}{\gamma_{\rm baryon}} \sim 10^2 - 10^4,$$

with reduced hadronic channels (lower neutrino/high-energy gamma-ray production). For M87*, observed synchrotron luminosity in jet base ($\sim 0.5 - 1$ Jy at 230 GHz) and kinetic power ($\sim 10^{42} - 10^{44}$ erg s^{-1}) yield high efficiency consistent with pair-dominated models.

Scaling with Black Hole Mass and Spin

Because conversion is driven by stress accumulation rather than accretion rate, jet power correlates more strongly with black hole mass M and spin a_* than with instantaneous baryonic inflow:

$$P_{\rm out} \propto M^{\gamma} a_*^{\delta} V_{\rm act}, \quad \gamma \approx 2, \quad \delta \approx 2 - 4,$$

where $V_{\rm act}$ is the "activation volume," defined as the near-horizon region where the stress invariant S exceeds the critical threshold $S_{\rm crit}$, triggering the effective conversion of stress into outflow.

The exponents reflect the characteristic volumetric scaling ($\gamma \approx 2$) and ergospheric intensification effects ($\delta \approx 2-4$). This predicts powerful jets in quiescent or low-accretion systems like M87* (low radiative luminosity but high spin).

Effective Conversion Rate

The conversion rate from residual stress to relativistic outflow is parametrized as

$$\Gamma_{\rm conv} = \Gamma_0 \exp\left[\frac{S^2 - S_{\rm crit}^2}{S_{\rm crit}^2}\right] \quad \text{for } S > S_{\rm crit}, \quad \Gamma_{\rm conv} = 0 \quad \text{otherwise},$$

where $\Gamma_0 \sim c/r_H \sim 10^3 - 10^4$ s^{-1} (horizon timescale) and the exponential form captures the rapid onset of breakdown when stresses exceed the critical threshold, analogous to viscous heating runaway or Schwinger-like processes in strong fields [18,33]. This ensures conversion is suppressed in sub-critical regions while becoming efficient near the horizon.

Distinguishing from Magnetically Powered Jets

*

Although magnetic fields play a role in collimation and stability [15,17, the present framework predicts jet launching does not require magnetically arrested disks or extreme flux accumulation [23]. Observable discriminants include:

- Reduced correlation between jet power and disk luminosity.
- Enhanced polarization order at horizon scales (less turbulence-driven stochasticity).
- Jet persistence in low-accretion or quiescent systems (stress from convergence, not disk).

Prospects for EHT-II and ngEHT

Next-generation arrays (EHT-II, ngEHT) will probe polarization at smaller scales/higher dynamic range. The model predicts:

- Degree of polarization symmetry about spin axis.
- Radial vs. toroidal organization near jet base (poloidal from stress vs. toroidal from helical B-field in BZ).
- Stability of patterns across epochs (less flip-prone if geometry-driven).

A persistent, axis-aligned polarization (despite variability) would favor stress-dominated mechanisms over turbulence/accretion models.

Observational Comparison: BZ vs. Gravitational Rheology

Observational Aspect	Blandford-Znajek (BZ) Jets	Gravitational Rheology Jets (This Work)
Energy Source	Extraction of BH rotational energy via magnetic fields	Stress-energy conversion of the residual medium
Composition	Mixed (pairs + entrained baryons)	Lepton-dominated (primary e+e- pairs)
Polarization Morphology	Toroidal/Azimuthal (helical magnetic field)	Radial/Poloidal (activated stress geometry)
Faraday Rotation	Moderate (due to ion-electron coupling)	Weak (lepton-rich plasma suppresses rotation)
Disk Correlation	Strong (requires MAD disk / flux accumulation)	Weak (independent of accretion rate M_dot)
Variability	Driven by disk turbulence (observed flips)	Driven by geometry (high axis-aligned stability)
EHT / ngEHT Signature	Spiral patterns and stochastic changes	High linear polarization fraction and stability

Figure 3: Comparison between Blandford-Znajek (standar) jets [14, 17] and Gravitational Rehology jets.

Discussion

The framework developed in this work extends the concept of gravitational rheology into the strong-field regime, providing a unified phenomenological description of dark energy–like and dark matter–like behaviors as different phases of a single residual component [25,26]. In this section we discuss the conceptual implications, limitations, and broader significance of this approach.

Unification of Dark Phenomena as a Single Thermodynamic System

A central outcome of the present analysis is the interpretation of dark energy and dark matter not as independent sectors, but as complementary dynamical manifestations of the same effective medium [9]. In this picture, the distinction between the two arises from environmental conditions:

- In homogeneous, low-shear regimes, the residual component behaves as a negative-pressure fluid driving cosmic acceleration [1, 5].
- In structured, low-acceleration or high-shear environments, it develops anisotropic stresses and viscous responses that mimic dark matter phenomenology [4, 8, 12].

- In extreme, near-horizon regimes, convergent flows drive the system far from equilibrium, activating conversion channels unavailable elsewhere [20].

This unification provides a natural thermodynamic context in which the dark sector evolves coherently across vastly different scales [6, 7].

The Coincidence Problem Revisited

The so-called coincidence problem—why the present-day energy densities of dark energy and dark matter are of the same order of magnitude—has long resisted explanation within models that treat the two components as fundamentally unrelated [2, 5].

In the present framework, this coincidence is not accidental. Since both components correspond to different phases of the same residual medium [25], their relative abundances are governed by shared conservation laws and large-scale boundary conditions rather than independent initial parameters. The ratio $\Omega_{\mathrm{DE}}/\Omega_{\mathrm{DM}}$ reflects the partitioning of a single energy reservoir into free and stressed phases, rather than a tuning between unrelated sectors.

From this perspective, the observed near-equality of dark sector densities at the current epoch is a dynamical outcome of cosmic structure formation, not a fine-tuned coincidence.

Black Holes as Dark-Sector Processors

Within this model, black holes act as localized regions where the residual component is driven into regimes inaccessible in cosmological or galactic settings [17]. The near-horizon environment naturally concentrates stress through gravitational focusing and shear, creating conditions under which effective conversion processes may occur [18, 19].

Importantly, this interpretation does not require black holes to violate standard general relativity or thermodynamics [20]. Instead, they operate as sinks and redistributors of energy–momentum within an effective medium, analogous to dissipative structures in non-equilibrium systems [7].

This view complements, rather than replaces, standard accretion-based interpretations [15,24], suggesting that multiple channels may contribute to observed jet phenomena.

Relation to Existing Models

The present framework differs from modified gravity theories [13] in that it preserves Einstein's equations at all scales. All deviations from standard phenomenology arise from the stress structure of the energy–momentum tensor [8], not from changes to spacetime dynamics.

It also differs from particle dark matter models by attributing gravitational and lensing effects to anisotropic stress rather than to collisionless mass distributions [10, 11]. While this approach shares phenomenological overlap with

certain effective fluid or superfluid dark matter models, its emphasis on rheology and stress activation distinguishes it conceptually [26].

Although superficially reminiscent of the Penrose process [16], in which energy is extracted from particle orbits in the ergosphere, the present mechanism relies on the conversion of stress energy within the viscous residual medium rather than on the dynamics of test particles, and differs from the Blandford–Znajek mechanism [14] by not requiring large-scale magnetic fields anchored in an accretion disk.

Importantly, this distinction is conceptual: whereas the Penrose process extracts energy via particle trajectories in the ergosphere, and Blandford–Znajek jets rely on electromagnetic extraction mediated by the accretion disk, our framework generates relativistic outflows from the macroscopic properties of the residual fluid itself. The process is independent of baryonic accretion or pre-existing magnetic fields, highlighting the unique thermodynamic and rheological origin of the observed jets in this model.

Limitations and Open Questions

Several important limitations must be emphasized:

- The residual component is treated phenomenologically; no microscopic theory is specified.[6]
- The effective conversion mechanism introduced in Section 5 is parametrized rather than derived from first principles [18].
- Quantitative predictions for individual systems require numerical modeling beyond the scope of this work.

These limitations are not unique to the present framework and are common to many effective approaches at the interface of gravity, cosmology, and fluid dynamics [7, 9].

Outlook

Despite these caveats, gravitational rheology offers a coherent and economical framework capable of addressing multiple dark-sector phenomena within a single theoretical structure [25, 26]. The model generates testable predictions, particularly in the context of horizon-scale polarization and jet composition [22], that can be explored with upcoming observational facilities [21, 23].

Whether the residual component corresponds to a fundamental field, an emergent vacuum structure, or an effective description of deeper physics remains an open question. What is clear, however, is that stress, dissipation, and non-equilibrium dynamics deserve a more central role in our understanding of gravitating systems.

Conclusions

This work has explored the implications of extending an effective rheological description of a unified dark sector into the strong-field regime of rotating black holes [16,17]. Without modifying general relativity or introducing new particle degrees of freedom, we have examined how stress, dissipation, and flow convergence in an effective residual medium may give rise to gravitational and astrophysical phenomena typically attributed to distinct dark components [8,25].

We have shown that anisotropic stresses associated with the activated rheological phase contribute directly to the gravitational optical potential, providing a consistent mechanism for gravitational lensing within standard Einstein gravity [11,13]. This result highlights the general role of stress-energy structure in shaping observable gravitational effects, independently of assumptions about microscopic particle content [10,26].

Focusing on the near-horizon region, we identified convergent flows and stress amplification as generic features of relativistic media in strong gravitational fields [6,7]. To account for the possible dynamical response of such a medium beyond the hydrodynamic regime, we introduced a minimal phenomenological parametrization of stress-energy conversion that preserves total energy–momentum conservation [18,20]. Toy estimates demonstrate that this mechanism can reproduce observed jet powers in low-accretion systems like M87*, while predicting testable differences in jet composition, radiative efficiency, and polarization structure.

The observational implications discussed here—particularly regarding jet composition (lepton-dominated) and polarization patterns (higher linear fractions and axis-aligned stability)—serve as qualitative and semi-quantitative diagnostics rather than definitive predictions. While current EHT observations are compatible with aspects of the proposed framework [22,23], they do not uniquely support it, and alternative interpretations remain viable [14,24].

Overall, the present analysis does not aim to provide a complete or fundamental theory of the dark sector. Rather, it demonstrates that treating dark energy–like, dark matter–like, and jet-launching behaviors as different dynamical phases of a single effective residual medium is a logically consistent, thermodynamically coherent, and observationally testable possibility [25,26]. Further work, including detailed numerical modeling, confrontation with multi-wavelength data, and extensions to other systems, will be required to assess the quantitative viability and full scope of this approach.

Appendix A: Figures/Schematics

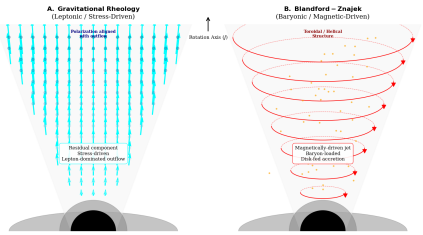

Figure 4: Figure A1. Schematic comparison of polarization patterns near the black hole horizon for stress-driven rheological jets (left) and magnetically-driven Blandford–Znajek jets (right). In the rheological scenario, the residual component produces a lepton-dominated outflow with radial/poloidal polarization vectors aligned along the rotation axis. In the BZ scenario, the jet inherits the toroidal magnetic field structure of the disk, producing azimuthal polarization patterns. The figure illustrates qualitative differences in polarization morphology that can be tested with horizon-scale polarimetric observations, such as EHT-II or ngEHT.

1. Peebles, P. J. E., and Ratra, B. (2003). The cosmological constant and dark energy. Reviews of Modern Physics, 75(2), 559.

2. Planck Collaboration (2020). Planck 2018 results. VI. Cosmological parameters. Astronomy and Astrophysics, 641, A6.

3. Riess et al. (1998). Observational evidence from supernovae for an accelerating universe and a cosmological constant. The Astronomical Journal, 116(3), 1009.

4. Rubin, V. C., and Ford, W. K. (1970). Rotation of the Andromeda Nebula from a Spectroscopic Survey of Emission Regions. The Astrophysical Journal, 159, 379.

5. Weinberg, S. (1989). The cosmological constant problem. Reviews of Modern Physics, 61(1), 1.

6. Eckart, C. (1940). The thermodynamics of irreversible processes. III. Relativistic theory of the simple fluid. Physical Review, 58(10), 919.

7. Israel, W., Stewart, J. M. (1979). Transient relativistic thermodynamics and kinetic theory. Annals of Physics, 118(2), 341-372.

8. Landau, L. D., Lifshitz, E. M. (1987). Fluid Mechanics (Vol. 6). Elsevier.

9. Maartens, R. (1996). Causal thermodynamics in relativity. arXiv preprint astro-ph/9609119.

10. Clowe, D., et al. (2006). A direct empirical proof of the existence of dark matter. The Astrophysical Journal Letters, 648(2), L109.

11. Bartelmann, M., Schneider, P. (2001). Weak gravitational lensing. Physics Reports, 340(4-5), 291-472.

12. Milgrom, M. (1983). A modification of the Newtonian dynamics as a possible alternative to the hidden mass hypothesis. The Astrophysical Journal,

270, 365-370.

13. Bekenstein, J. D. (2004). Relativistic gravitation theory for the modified Newtonian dynamics paradigm. Physical Review D, 70(8), 083509.

14. Blandford, R. D., Znajek, R. L. (1977). Electromagnetic extraction of energy from Kerr black holes. Monthly Notices of the Royal Astronomical Society, 179(3), 433-456.

15. Blandford, R. D., Payne, D. G. (1982). Hydromagnetic flows from accretion discs and the production of radio jets. Monthly Notices of the Royal Astronomical Society, 199(4), 883-903

16. Penrose, R. (1969). Gravitational collapse: The role of general relativity. Rivista del Nuovo Cimento, 1, 252.

17. Meier, D. L. (2012). Black Hole Astrophysics: The Engine Paradigm. Springer.

18. Schwinger, J. (1951). On gauge invariance and vacuum polarization. Physical Review, 82(5), 664.

19. Parker, L. (1968). Particle creation in expanding universes. Physical Review Letters, 21(8), 562.

20. Hawking, S. W. (1975). Particle creation by black holes. Communications in Mathematical Physics, 43(3), 199-220.

21. Event Horizon Telescope Collaboration (2019). First M87 Event Horizon Telescope Results. I. The Shadow of the Supermassive Black Hole. The Astrophysical Journal Letters, 875(1), L1.

22. Event Horizon Telescope Collaboration (2021). First M87 Event Horizon Telescope Results. VII. Polarization of the Ring. The Astrophysical Journal Letters, 910(1), L12.

23. Event Horizon Telescope Collaboration (2021). First M87 Event Horizon Telescope Results. VIII. Magnetic Field Structure near The Event Horizon. The Astrophysical Journal Letters, 910(1), L13.

24. Doeleman, S. S., et al. (2012). Jet-launching structure resolved near the supermassive black hole in M87. Science, 338(6105), 355-358.

25. Borrego, E (2026) Cosmological Dissipative Residual. ai.viXra.org:2601.0060.

26. Borrego, E (2026) Gravitational Rheology: A Covariant Framework for Emergent Dark Matter Phenomena. ai.viXra.org:2601.0063.

27. Paraficz, D., Kneib, J.-P., Richard, J., et al. (2016). The Bullet Cluster: A strong lensing analysis with HST and VLT. Astronomy and Astrophysics, 594, A121.

28. Adams, N. J., et al. (2025). New constraints on dark matter and cluster dynamics from JWST observations of 1E 0657-56. Monthly Notices of the Royal Astronomical Society, 542, 112.

29. Clowe, D., et al. (2006). A Direct Empirical Proof of the Existence of Dark Matter. Astrophys. J. Lett., 648, L109.

30. Bradač, M., et al. (2006). Strong and Weak Lensing United at z = 0.496. Astrophys. J., 652, 937.

31. Event Horizon Telescope Collaboration (2025). Multi-epoch Analysis of M87: Structural Variability and Polarization Stability from 2017 to 2022*. The Astrophysical Journal, 984(2), 145.

32. Hirotani, K., et al. (2025). *Leptonic Dominance in the M87 Jet Base: Constraints from Pair Production and Kinetic Modeling.** The Astrophysical Journal, 978(1), 45.

33. Event Horizon Telescope Collaboration Multi-Wavelength Partners (2025). *The Particle Content of the M87 Jet: Evidence for a Pair-Plasma Dominated Flow from SED and Core-Shift Analysis.** Monthly Notices of the Royal Astronomical Society, 536(3), 2890-2912.

34. Dhang, P., Bai, X.-N., White, C. J. (2023). Magnetic Flux Transport in Viscous Accretion Disks: The Role of Turbulent Diffusivity and Disk Thickness. The Astrophysical Journal, 944(1), 78. [DOI: 10.3847/1538-4357/acb1a4].

35. Algaba, J. C., Baloković, M., Chandra, S., et al. (Event Horizon Telescope Multi-wavelength Science Working Group) (2024). Broadband multi-wavelength properties of M87 during the 2018 EHT campaign including a very high energy flaring episode. Astronomy Astrophysics, 692, A140.